Electronic Supplementary Information

A facile self-saturation process enabling the stable cycling of a small molecule menaquinone cathode in aqueous zinc batteries

Shuo Li[a], Guoli Zhang [a,*], Qianrui Li[a], Tianshun He[a] and Xiaoqi Sun [a,b,*]

[a.] Department of Chemistry, Northeastern University, Shenyang 110819, China.

[b.] National Frontiers Science Center for Industrial Intelligence and Systems Optimization, Northeastern University, 3-11 Wenhua Road, Shenyang, 110819, China.

*Corresponding authors.

E-mail: 2210076@stu.neu.edu.cn; sunxiaoqi@mail.neu.edu.cn

1 Experimental procedures

1.1 Materials.

Naphthoquinone (NQ) and menaquinone (Me-NQ) were purchased from Aladdin Bio-Chem Technology (China). Carbon paper was purchased from the SGL group (Germany). Ketjen Black (KB) conductive additive was purchased from Lion Specialty Chemicals (Japan). Polytetrafluoroethylene (PTFE) was purchased from Daikin Industries (Japan). The other reagents were obtained from Sinopharm Chemical Reagent (China).

1.2 Material characterizations.

X-ray diffraction (XRD) was performed on a PANalytical Empyrean diffractometer with Cu Kα radiation as the X-ray source. The morphology was obtained on a scanning electron microscope equipped with an energy dispersive X-ray spectroscopy (EDS) detector (HITACHI, SU8010, Japan). Fourier transform infrared (FT-IR) spectroscopy was measured on VERTEX70 (Bruker, Germany). UV-vis spectra were obtained by a Lambda XLS+ UV-vis spectrometer. Nuclear magnetic resonance (NMR) was measured with Bruker 400M.

1.3 Electrochemical measurements

The electrodes were prepared by mixing Me-NQ or NQ active material, KB carbon, and PTFE binder at the mass ratio of 5:4:1 in the mixed solvent of water:ethanol = 15:1 (volume ratio). The slurry was drop cast on carbon paper substrate and dried at room temperature overnight. The mass loading of active material was around 1.1 mg cm^{-2}, except for the study of the cathode with high mass loading around 4 mg cm^{-2}. Coin-type batteries were assembled with 2 M $ZnSO_4$ electrolyte. The self-discharge tests were performed by cycling the cathode for 3 cycles at 0.1 A g^{-1}, stopped at 1.5 V and rested for 48 h, followed by a discharge at 0.1 A g^{-1}. Electrochemical impedance spectroscopy (EIS) was conducted in the frequency range from 100 kHz to 100 mHz with an amplitude of 5 mV. Galvanostatic intermittent titration technique (GITT) was carried out with the current pulse of 0.05 A g^{-1} for 30 min, followed by 3 h relaxation. The diffusion coefficient D (cm^2 s^{-1}) was calculated according to the following formula:[1]

$$D^{GITT} = \frac{4}{\pi\tau}\left(\frac{m_B V_M}{M_B S}\right)^2 \left(\frac{\Delta E_S}{\Delta E_\tau}\right)^2 \quad (1)$$

The τ, m_B, V_M, M_B, and S were the pulse period, mass, molar volume, molar mass, and geometric surface area of the electrode, respectively. ΔE_S was the potential change during relaxation, and ΔE_τ represented the potential change during a pulse after excluding the IR drop. All electrochemical measurements were carried out on Bio-Logic VMP3 or LAND-CT2001A battery test systems.

1.4 Computational details.

Density functional theory (DFT) calculations were carried out with the Gaussian 16 software package. Geometrical optimizations were conducted with Becky's three-parameter exchange function combined with the Lee-Yang-Parr correlation functional (B3LYP) method and 6-31 G (d) basis set. The binding energies (E_b) between Me-NQ and different cations were calculated based on the following equation:

$$E_b = E_{(Me-NQ+cations)} - E_{(cations)} - E_{(Me-NQ)} \quad (2)$$

$E_{(Me\text{-}NQ+cations)}$, $E_{(cations)}$ and $E_{(Me\text{-}NQ)}$ were the energies of Me-NQ after coordinated with Zn^{2+}/H^+ cations, Zn^{2+}/H^+ cations and Me-NQ, respectively.

2 Supplementary Figures and Table

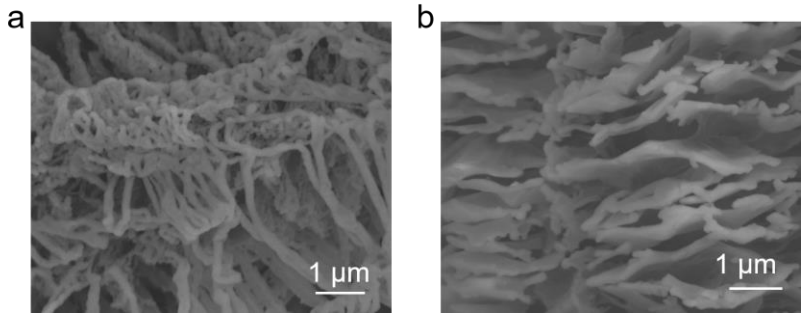

Figure S1. SEM images of a) NQ and b) Me-NQ.

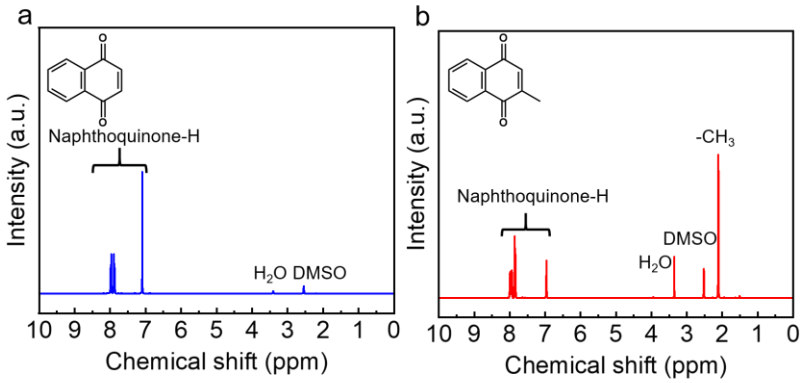

Figure S2. NMR of a) NQ and b) Me-NQ.

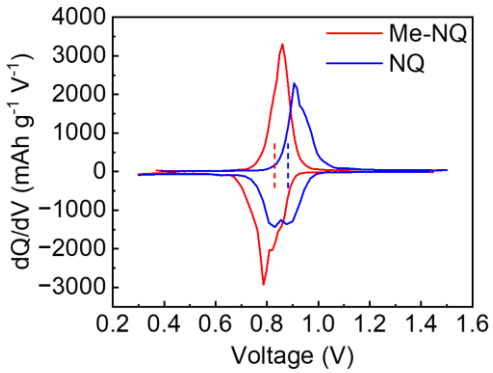

Figure S3. Differential capacity curves of NQ and Me-NQ at 0.1 A g^{-1} (the blue and red dashed lines represent the average redox voltages for NQ and Me-NQ, respectively).

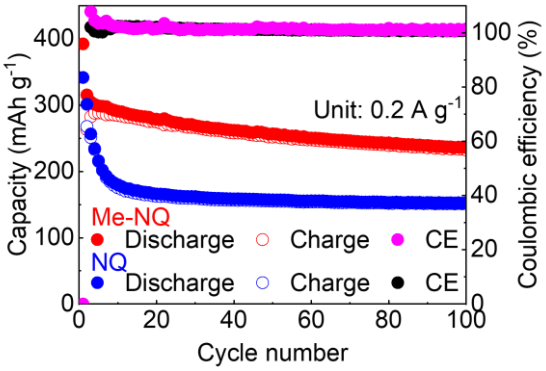

Figure S4. Cycling performance of Me-NQ and NQ at 0.2 A g^{-1}.

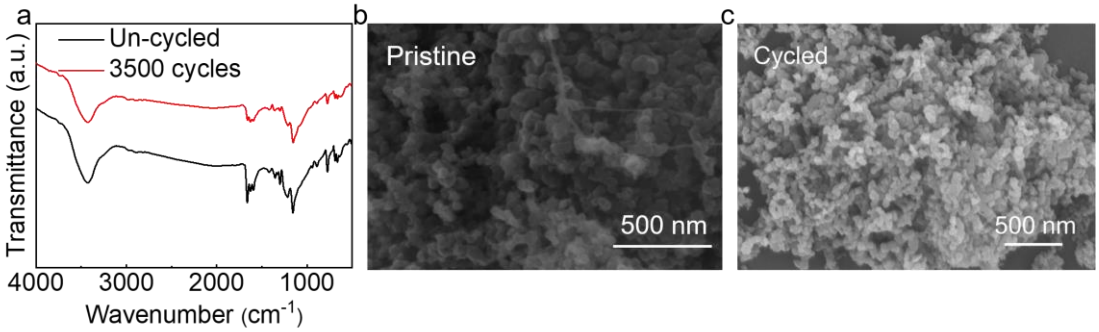

Figure S5. a) FT-IR of the pristine Me-NQ cathode and after 3500 cycles at 5 A g^{-1}. SEM images of b) the pristine Me-NQ cathode and c) after 3500 cycles at 5 A g^{-1} (the morphology of active material changed during electrode preparation and it was uniformly mixed with carbon additive).

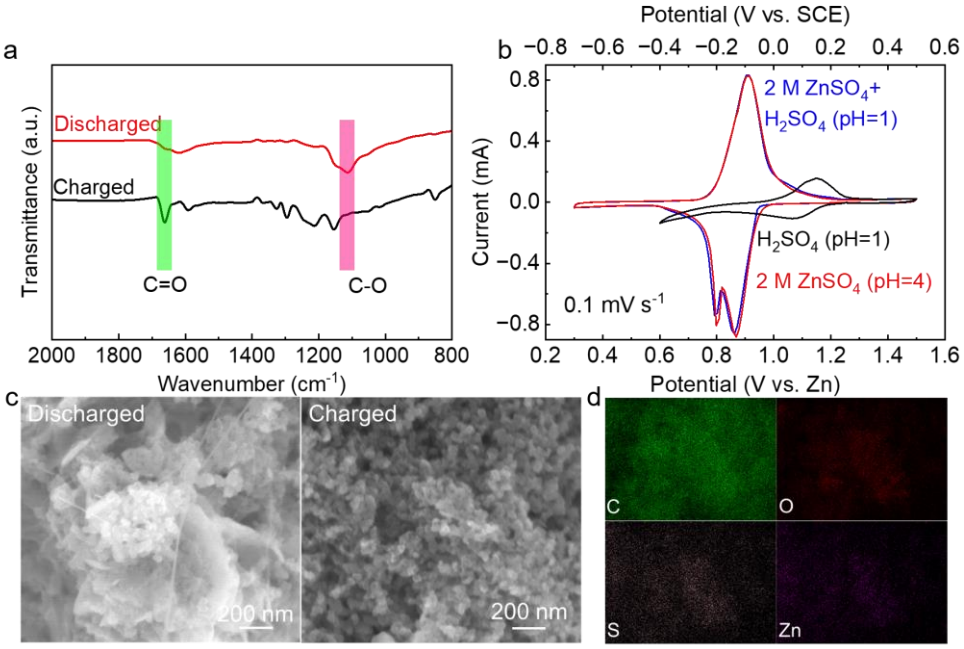

Figure S6. a) FT-IR of NQ at different states. b) CV of NQ in different electrolytes at 0.1 mV s^{-1}. c) SEM images of NQ at different states. d) EDS mappings of the discharged NQ.

Table S1. Cycling performance comparison of Me-NQ cathode with previously reported organic cathode materials in aqueous zinc batteries.

Cathode	Electrolyte	Current density	Cycle number	Capacity retained after cycling	Ref.
Lignin@C	PAAK+0.2 m $Zn(TFSI)_2$	1 A g^{-1}	8000	37 mAh g^{-1}	2
P($4VC_{86}$-stat-SS_{14})	4 M $Zn(TFSI)_2$	30 C	48000	184 mAh g^{-1}	3
PC/G-2	3 M $ZnSO_4$	2 C	3000	158 mAh g^{-1}	4
TAHQ	2 M $ZnSO_4$	5 A g^{-1}	1000	99 mAh g^{-1}	5
TRT	2 M $ZnSO_4$	0.5 A g^{-1}	1000	65 mAh g^{-1}	6
PMTP@CNT-40	2 M $ZnSO_4$	3 A g^{-1}	4000	150 mAh g^{-1}	7
TA-PTO-COF	2 M $ZnSO_4$	1 A g^{-1}	1000	142 mAh g^{-1}	8
Me-NQ	2 M $ZnSO_4$	5 A g^{-1}	3500	146 mAh g^{-1}	This work

3 References

1. Y. Chen, C. Lin, X. Chen, Z. Lu, K. Zhang, Y. Liu, J. Wang, G. Han, and G. Xu, Modulating the Structure of Interlayer/Layer Matrix on $\boldsymbol{\delta}$-MnO_2 via Cerium Doping-Engineering toward High-Performance Aqueous Zinc Ion Batteries, *Adv. Energy Mater*., 2024, **14**, 2304303.
2. D. Kumar, L. R. Franco, N. Abdou, R. Shu, A. Martinelli, C. M. Araujo, J. Gladisch, V. Gueskine, R. Crispin and Z. Khan, Water-in-Polymer Salt Electrolyte for Long-Life Rechargeable Aqueous Zinc-Lignin Battery, *Energy Environ. Mater.,* 2024, DOI: 10.1002/eem2.12752.
3. N. Patil, C. de la Cruz, D. Ciurduc, A. Mavrandonakis, J. Palma and R. Marcilla, An Ultrahigh Performance Zinc-Organic Battery using Poly(catechol) Cathode in $Zn(TFSI)_2$-Based Concentrated Aqueous Electrolytes, *Adv. Energy Mater.*, 2021, **11**, 2100939.
4. S. Zhang, W. Zhao, H. Li and Q. Xu, Cross-Conjugated Polycatechol Organic Cathode for Aqueous Zinc-Ion Storage, *ChemSusChem*, 2020, **13**, 188-195.
5. Y. Wang, S. Niu, S. Gong, N. Ju, T. Jiang, Y. Wang, X. Zhang, Q. Sun and H.-b. Sun, Fused Functional Organic Material with the Alternating Conjugation of Quinone-Pyrazine as Cathode for Aqueous Zinc Ion Batteries, *Small Methods*, 2024, **8**, 2301301.
6. W. Wang, Y. Tang, J. Liu, H. Li, R. Wang, L. Zhang, F. Liang, W. Bai, L. Zhang and C. Zhang, Boosting the Zinc Storage of a Small-Molecule Organic Cathode by a Desalinization Strategy, *Chem. Sci.*, 2023, **14**, 9033-9040.
7. Y. Liu, Z. Li, C. Li, Y. Wei, S. Yan, Z. Ji, S. Zou, H. Li, Y. Liu, C. Chen, X. He and M. Wu, Imidazole-Linked Covalent Organic Polymers with Abundant Oxygen and Nitrogen Active Centers for Advanced Aqueous Zinc-Organic Batteries, *Chem. Eng. J.*, 2024, **488**, 150778.
8. H. Li, M. Cao, Z. Fu, Q. Ma, L. Zhang, R. Wang, F. Liang, T. Zhou and C. Zhang, A Covalent Organic Framework as a Dual-Active-Center Cathode for a High-Performance Aqueous Zinc-Ion Battery, *Chem. Sci.*, 2024, **15**, 4341-4348.